Original Article
Bulletin of Pure and Applied Sciences.
Mathematics & Statistics Vol.43 E, No.2.
July-December 2024: P.118-132

Print version ISSN 0970 6577
Online version ISSN 2320 3226
Available online at www.bpasjournals.com

Numerical Investigation of Nanofluid MHD Flow across an Extended Stretching Sheet with Slip and Darcy Dissipation

[1]M. Mallick, and [2]S. Kar *

Author Affiliation:
[1,2]Dept. of Mathematics, DRIEMS University, Cuttack, Odisha 754022, India.

***Corresponding Author: S. Kar,** Dept. of Mathematics, DRIEMS University, Cuttack, Odisha 754022, India.
E-mail: satyabratkr@gmail.com

Received on 15.08.2024, Revised on 11.10.2024, Accepted on 15.11.2024

ABSTRACT
The flow of thermoradiative nanofluids on an elongating surface is tested in this work using porous media. The flow dynamics are influenced by the combined effects of the thermally dependent and exponential heat sources. In addition, magnetic impacts have been applied to the inclined flow system. On the other hand, Darcy dissipation and a heat source have been used to study heat transfer in the unsteady MHD Nanofluid slip flow over an inclined stretching sheet. The study gains interest when the Soret number is present. The similarity transformation technique is used to transform the leading partial differential equations into a small number of ordinary differential equations. The reduced system is addressed using the 4th order R-K method with shooting technique.

Keywords: Darcy Dissipation, Nanofluid, Inclined Magnetic Field, Porous Media, Heat Source, Slip Conditions, Shooting Technique.

How to cite this article: M. Mallick, S. Kar (2024). Numerical Investigation of Nanofluid MHD Flow across an Extended Stretching Sheet with Slip and Darcy Dissipation. *Bulletin of Pure and Applied Sciences- Math & Stat.*, 43E (2), 118-132.

1. Introduction

Nanofluids are composed with combination of nanoparticles and pure fluid, where both are mixed together. The accumulation of nanoparticles significantly alters the thermal, optical, and rheological features of the base fluid, resulting in nanofluids with enhanced heat transfer capabilities associated to conventional fluids as noticed by Choi and Eastman [1]. Achieving stable dispersion and preventing particle agglomeration are critical challenges in nanofluid synthesis and application, often addressed through surface modification, surfactants, or stabilizers. Nanofluids ,which considering in several industries and thermal management of electronics, heat exchangers, solar energy systems, automotive cooling, and biomedical devices, owing to their superior heat transfer performance and potential for tailored properties [2,3].

Hybrid nanofluid flow represents a cutting-edge area of research in thermal engineering, where the introduction of several kinds of nanoparticles into a pure fluid creates a composite fluid with enhanced heat transfer properties [4]. This innovative approach capitalizes on the synergistic effects of combining different nanoparticle materials, such as metallic and non-metallic particles, to tailor the fluid's thermal conductivity, viscosity, and other key characteristics for specific applications. The impacts of hybrid

nanofluid flow on heat transfer phenomena are profound and multifaceted [5,6]. Alharbi et al. [7] investigated the thermal management for nanofluid flow through the annular region affected by radiative and magnetized process. Animasaun et al. [8] discussed time-dependent trihybrid nanofluid flow on a stretching sheet with impacts of bio-convection and thermal conductance of nanoparticles. Bani-Fawaz et al. [9] discussed computationally the thermal flow phenomenon for radiated nanoparticles flow influenced by diameter of molecule and features of nanoparticles.Rawat et al. [10] used non-Fick and non-Fourier phenomena to investigate mixed convective MHD flow of liquid on a flat surface under convective thermal constraints at the boundaries. Abrar [11] discussed the production of entropy for dual diffusive tangential hyperbolic fluid flow on a stretchable sheet of Darcy medium with impacts of slip factors and viscous dissipation. Experimental and practical studies have established that the numerical and semi-analytical approaches on MHD Nanofluid flow in natural convection heated lid-driven square cavity filled with Fe3O4-water presented by scientists ([12]-[14]).M. Sheikholeslami et al. [15] have investigated the nanofluid flow with heat transfer between parallel plates assuming Brownian motion. Saleem et al. [16] inspected the perception of nanofluid flow by discussing the impacts of different kinds of nanoparticles and their shapes on fluid flow past a horizontal surface and have proved that growth rate of Brownian factor has resulted a reduction in thermal distribution. Cao et al. [17] simulated the dynamics of trihybrid nanoparticles flow and have noticed that with growth in concentration of nanoparticles there has been an augmentation in thermal distributions. Abrar et al. [18] inspected computationally the production of entropy for MHD Casson fluid flow on a wedge and have observed that velocity distribution of fluid has augmented with escalation in wedge angle factor and Casson parameter.

This force exerts a deflecting influence on the fluid flow, leading to alterations in velocity profiles, flow patterns, and shear stresses within the fluid. These changes, in turn, profoundly affect the mechanisms of convective heat transfer [19]. Forced convection, driven by external forces or pressure gradients, experiences modifications due to the Lorentz force induced alterations in flow direction and velocity distribution. Similarly, natural convection, driven by buoyancy forces resulting from temperature gradients, undergoes significant transformations with effect of inclined magnetic field [20]. Khan et al. [21] discussed transportation analysis for mixed convective squeezed flow of Casson fluid on an inclined stretchable surface using the impacts of dual stratifications. Recently, the huge development with greater impact of magnetic field on nanofluids has also been investigated by other eminent researchers (S.Nadeem et al. [22], C.S.K. Raju et al. [23], Kai-Long Hsiao [24], and S.S. Ghadikolaei et al. [25]). In such scenarios, slip alters the velocity profile near the boundary, influencing the convective heat transmission rate and temperature distribution within the liquid [26]. The presence of slip can lead to enhanced or reduced heat transfer rates depending on factors such as the slip length, fluid properties, and geometry. At micro- and nanoscales, where slip effects become increasingly significant, understanding the relationship between fluid flow with slip conditions and thermal transport is crucial for various applications. For instance, in microfluidic heat exchangers, slip-induced changes in flow behaviour can impact heat transfer efficiency and overall device performance. Similarly, in nanoscale thermal management systems, such as heat dissipation in electronic devices, slip conditions may affect temperature gradients and heat transfer rates, influencing device reliability and performance [27].

In Magnetohydrodynamics (MHD) with electrically conductive fluid flows, due to its frequent application in various fields like science, engineering and industrial sectors. It has been used in MHD power generation, MHD pumps, MHD flow in nanofluids, manufacturing and heterogeneous composition in food, atmospheric density stratification etc. In view of these widely applications drawn the attentions of some researchers (D.D. Ganji et al.[28], M. Hatami et al.[29], S.M. Ibrahim et al. [30], S.S. Ghadikolaei et al. [31] and Umar Khan et al.[32]) to explore their perceptions, pondering, speculation and ideas in these directions. An inclined magnetic field refers to a field whose direction deviates from being perfectly horizontal or vertical. In such scenarios, the Lorentz force, arising from the collaboration between the conducted (electrically) fluid and magnetic field, becomes a dominant factor in determining the flow dynamics [33,34]. E.Haile et al. [35] have developed a nanofluid model for analysing the thermophoresis diffusion, thermal energy transport etc. with the Brownian motion of nanofluids.

The Outstanding and reliable techniques to address the high nonlinear problems , Partial differential equations are transformed into ordinary differential equations using the leading Similarity transformation, and numerical solutions are obtained using the fourth order Runge-Kutta method with shooting technique. This method has adopted to get through the numerical solutions of non-linear dynamic problems. Kar S. Senapati N., Swain B.K [36] reviewed critically the augmentation of thermal transmission for the flow of nanoliquid on a porous media using the mechanism of microorganism.

Further, S.Kar et al. [37] have observed the analysis of fluid flow over an inclined plate with wall temperature and concentration. Chen CH et al.[38],[39]and S.Ahmed et al.[40] One common example is found in electronic devices, where the power dissipation within the device fluctuates due to varying operational conditions and computational demands. In this case, the heat generation not only changes over time but also exhibits spatial variations within the device, with certain regions experiencing higher heat fluxes than others Most recently The Soret and Dufour effects on mixed convection boundary layer flow across a vertical surface in a porous medium containing a visco-elastic fluid have been observed by numerous researchers, reported by Senapati.N et.al [41] and Paul.A [42]. Moreover, T. Hayat et.al [43] have considered the effect of transpiration on coupled heat and mass transfer in mixed convection over a vertical plate embedded in a saturated porous medium. Yih.Ka. [44] in their experimental research based on the various numerical as well as analytical methods for the solutions on MHD flow of an incompressible viscous dissipative fluid in an infinite vertical oscillating plate with constant heat flux have been duly examined.

Additionally, such understanding finds relevance in various natural phenomena and industrial processes, such as geophysical fluid dynamics, metallurgical processes, and the operation of MHD systems in fusion reactors and space propulsion technologies. Researchers strive to unravel the complex mechanisms governing liquid flow and heat transport in inclined magnetic field configurations, aiming to enhance the reliability, efficiency, and sustainability of diverse engineering systems and processes. Swain.B.K et al. [45] examined convective slip fluid flow with double diffusive behaviour for nanofluid on an asymmetric conduit. K.Saeed et al. [46] inspected magnetized squeezed flow of nonlinearly stratified fluid flow with convective features and have observed that concentration and thermal distributions have declined with augmentation in thermal stratification. Q.Khan et al., Amer.A.M and Srihari.K et.al [47-49] studied slip effects on liquid flow due to elongating sheet with permeable impacts and have revealed that slip flow constraints significantly affects the flow phenomenon of the system. The study by B.K.Swain et al. [50] focused on time-dependent nanofluid flow influenced by slip conditions.

This study is diving head-first into the boundary layer flow over an elongated, stretchy sheet to figure out what's happening with thermal radiation, chemical reactions, the Soret effect, and even joule heating. We're using the snazziest numerical shooting technique around, complete with the fourth-order Runge-Kutta scheme, to crack the code of this particular physical model.

Now, let's talk parameters! We're unpacking everything from the diffusion coefficient to thermal conductivity, and even throwing in the magnetic field parameter for good measure. There's also radiative heat flux, mutual chemical reactions, and more porous media than you can shake a stick at. Unsteadiness parameter, Schmidt number, and Prandtl number also make the list, along with the Eckert number, thermal Grashof number, Solutal Grashof number, and last but not least, our pal, the Soret number. Let’s not forget velocity, temperature, concentration, and a special shout-out to skin friction and the Nusselt and Sherwood numbers. We're exploring all these parameters more thoroughly than a detective in a mystery novel, using graphs and tables to lay it all out neatly.

2. Formulation of Problem

In this problem we're dealing with two-dimensional unsteady MHD free convective flow of a viscous, incompressible, and radiating fluid prancing around on a stretching sheet. This performance features a cast of characters including external magnetic and electric fields, heat generation and absorption, thermal radiation, chemical reactions, viscous dissipation, and the legendary joule heating. Density changing with temperature and concentration, but only when it comes to body force. It's like density is a diva, only accepting roles where it can induce a buoyant force, causing all sorts of shenanigans with temperature and concentration levels A uniform magnetic field makes a daring entrance, striding perpendicularly to the stage. I mean, the surface of the stretching sheet. We've got a first-order chemical reaction partnering with thermal radiation take into consideration in this flow.

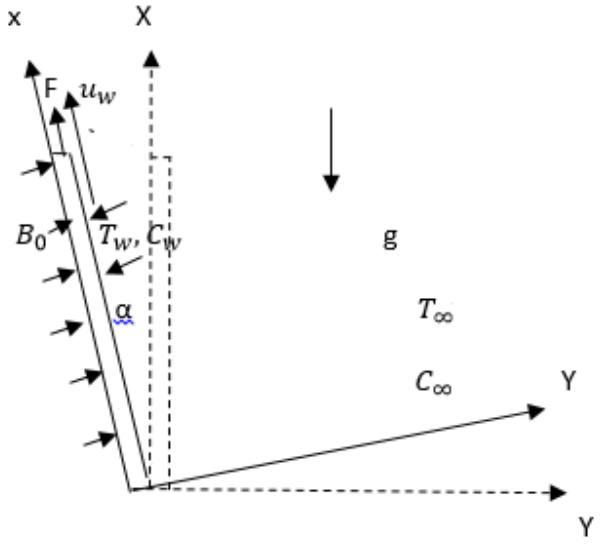

Figure 1: Graphical view of the flow phenomenon.

Let $u_w(x,t)$ be the velocity of the stretching sheet in the direction force F applied along in x-axis and the mass transfer $v_w(t)$. normal to the stretching sheet. We also assumed that surface temperature and concentration of the sheet are $T_w(x,t)$ and $C_w(x,t)$ respectively, in addition with T_∞ and C_∞ are the uniform temperature and concentration far from the sheet. We've got thermal conductivity and molecular diffusivity as linear functions of temperature. Imagine them strutting down a runway. And to top it off, we've got the Soret effects taking center stage with their fabulous characteristics of Soret effects are described.

The governing boundary layer equations are given below:-

$$\frac{\partial u}{\partial x}+\frac{\partial v}{\partial y}=0 \tag{1}$$

$$\frac{\partial u}{\partial t}+u\frac{\partial u}{\partial x}+v\frac{\partial u}{\partial y}= \nu^*\frac{\partial^2 u}{\partial y^2}-\frac{\nu^*}{k^*}u-\frac{\sigma B_0^2}{\rho}u+g\beta_T(T-T_\infty)cos\alpha+ g\beta_C(C-C_\infty)cos\alpha \tag{2}$$

$$\frac{\partial T}{\partial t}+u\frac{\partial T}{\partial x}+v\frac{\partial T}{\partial y}=\frac{1}{\rho C_P}\frac{\partial}{\partial y}\left(K(T)\frac{\partial T}{\partial y}\right)-\frac{1}{\rho C_P}\frac{\partial q_r}{\partial y}+\frac{\mu}{\rho C_P}\left(\frac{\partial u}{\partial y}\right)^2+\frac{\mu}{\rho C_P}\frac{u^2}{k^*}+Q^*(T-T_\infty) \tag{3}$$

$$\frac{\partial C}{\partial t}+u\frac{\partial C}{\partial x}+v\frac{\partial C}{\partial y}=\frac{\partial}{\partial y}\left(D(T)\frac{\partial C}{\partial y}\right)-K_C(C-C_\infty)+D_1\frac{\partial^2 T}{\partial y^2} \tag{4}$$

By using Boundary conditions

$u=u_w(x,t)=\frac{cx}{1-\lambda t}$,

$v=v_w(t)$,

$T = T_w(x,t)$,
$C = C_w(x,t)$, $\quad at \quad y = 0$
$u \to 0$,
$T \to T_\infty$,
$C \to C_\infty$, $\quad as \quad y \to \infty$ (5)

The Roseland's approximation, which is provided below, is used to model the radiation heat flux (q_r)

$$q_r = -\left(\frac{4\sigma^*}{3k_1}\right)\frac{\partial T^4}{\partial y} \quad (6)$$

Now, T^4 can be expressed as a linear combination of the temperature by expanding T^4 by Taylor's series about T_∞ to obtain (7):

$$T^4 = T_\infty^4 + 4T_\infty^3(T - T_\infty) + 6T_\infty^2(T - T_\infty)^2 + \cdots \quad (7)$$

$$T^4 \approx -3T_\infty^4 + 4TT_\infty^3 \quad (8)$$

Substituting, the result of T^4 from equation (8) into equation (6)

$$q_r = -\left(\frac{4\sigma^*}{3k_1}\right)\frac{\partial T^4}{\partial y} = -\left(\frac{4\sigma^*}{3k_1}\right)\frac{\partial}{\partial y}(-3T_\infty^4 + 4TT_\infty^3)$$

$$= -\left(\frac{16T_\infty^3\sigma^*}{3k_1}\right)\frac{\partial T}{\partial y} \quad (9)$$

$$\frac{\partial q_r}{\partial y} = -\left(\frac{16T_\infty^3\sigma^*}{3k_1}\right)\frac{\partial^2 T}{\partial y^2} \quad (10)$$

Substituting equation (10) into equation (3),it becomes

$$\frac{\partial T}{\partial t} + u\frac{\partial T}{\partial x} + v\frac{\partial T}{\partial y} = \frac{1}{\rho C_P}\frac{\partial}{\partial y}\left(K(T)\frac{\partial T}{\partial y}\right) + \frac{1}{\rho C_P}\left(\frac{16T_\infty^3\sigma^*}{3k_1}\right)\frac{\partial^2 T}{\partial y^2} + \frac{\mu}{\rho C_P}\left(\frac{\partial u}{\partial y}\right)^2 + \frac{\mu}{\rho C_P}\frac{u^2}{k^*} + Q^*(T - T_\infty) \quad (11)$$

The fluid concentration at the sheet's surface, $C_w(x,t)$ and its temperature at the sheet's surface, $T_w(x,t)$

$$T_w(x,t) = T_\infty + \frac{bx}{(1-\lambda t)^2}$$

$$C_w(x,t) = C_\infty + \frac{bx}{(1-\lambda t)^2} \quad (12)$$

Similarity Transformation technique: partial differential equations (PDEs) in equations (2), (4), and (11)— we're giving them a makeover into ordinary differential equations (ODEs), Introducing the dimensionless parameters$\eta = \sqrt{\frac{c}{\nu^*(1-\lambda t)}}\, y$, $\psi = \sqrt{\frac{\nu^* c}{(1-\lambda t)}}\, x f(\eta)$

$$\theta(\eta) = \frac{T - T_\infty}{T_w - T_\infty} \quad , \quad \phi(\eta) = \frac{C - C_\infty}{C_w - C_\infty} \quad (13)$$

and the relations given by (14):

$$T(x,t) = T_\infty + \frac{bx}{(1-\lambda t)^2}\,\theta(\eta)$$

$$C(x,t) = C_\infty + \frac{bx}{(1-\lambda t)^2}\,\phi(\eta) \quad (14)$$

Where $\nu^* = \frac{\mu}{\rho}$ is the free stream kinematic viscosity, $\psi(x,y)$ is a stream function which defines the velocity components in the form $u = \frac{\partial \psi}{\partial y} = \frac{cx}{(1-\lambda t)} f'(\eta)$,

$v = -\frac{\partial \psi}{\partial x} = -\sqrt{\frac{\nu^* c}{(1-\lambda t)}}\, f(\eta)$ by using those results, continuity equation (1) satisfied. Where as $f(\eta)$ represents injection and suction with the dimensionless space variable.

Additionally, θ(η) and ϕ(η) are dimensionless of the fluid's temperature and concentration, respectively. A function depicted in (15) allows the thermal conductivity of the nanofluid K(T) to change linearly with temperature:

$$\text{K (T)} = K_\infty \left(1 + \frac{\beta_1}{\Delta T}(T - T_\infty)\right) \quad (15)$$

and in terms of dimensionless temperature equation (15) reducing to equation (16) :

$$K(\theta) = K_\infty (1 + \beta_1 \theta) \quad (16)$$

Where $K(\theta)$ is the variation thermal conductivity with regard to dimensionless temperature. K_∞ is the fluid's thermal conductivity distance from the heated sheet, and β_1 is a tiny parameter that varies depending on the fluid's characteristics and indicates how quickly thermal conductivity changes with temperature.

Now the diffusion coefficient D (T) as a linear function of temperature shown below:

$$D(T) = D_\infty \left(1 + \frac{\beta_2}{\Delta T}(T - T_\infty)\right) \quad (17)$$

It may also be written in the form of dimensionless temperature as below:

$$D(\theta) = D_\infty (1 + \beta_2 \theta) \quad (18)$$

Where D (θ) is the variation diffusion coefficient with regard to dimensionless temperature. D_∞ is the fluid's diffusion coefficient far from the heated sheet, and β_2 is a tiny quantity that varies depending on the fluid's characteristics and indicates how quickly chemical diffusivity changes with temperature.

Now substituting the equations (12)-(14), (16) and (18), in equations (2), (4), (11) and (5) the following ordinary differential equations are obtained:

$$f''' = A\frac{\eta}{2} f'' + [A + Kp + M]f' + (f')^2 - ff'' - Gr\theta - Gc\phi \quad (19)$$

$$\theta'' = \frac{-\beta_1 \theta'^2 + \mathrm{Pr}[\mathrm{A}\left(\frac{\eta}{2}\right)\theta' + 2\mathrm{A}\theta + f'\theta - f\theta' - \mathrm{Ec}(f'')^2 - \mathrm{EcKp}f'^2 - \mathrm{Q}\theta]}{(1 + R + \beta_1\theta)} \quad (20)$$

$$\phi'' = \frac{-\beta_2(\theta'\phi') + \mathrm{Sc}[\mathrm{A}\left(\frac{\eta}{2}\right)\phi' + 2\mathrm{A}\phi + f'\phi - f\phi' + \mathrm{Kr}\phi - \mathrm{So}\theta'']}{(1 + \beta_2\theta)} \quad (21)$$

The initial and boundary conditions in dimensionless forms are

$$f(0) = f_w \ , f'(0) = 1 \ , \theta(0) = 1 \ , (0) = 1 \ , \quad \text{at } \eta = 0$$
$$f'(\eta) \longrightarrow 0 \ , \ \theta(\eta) \longrightarrow 0 \ , \ \phi(\eta) \longrightarrow 0 \ , \quad \text{as } \eta \longrightarrow \infty \quad (22)$$

The non-dimensional parameters A, Kp, M, Gr, Gc, Pr, R, Ec, Kr, Sc, and So are presented. According to the definition given in, these parameters stand for the following: unsteadiness, porous medium, magnetic, thermal, Grashof, solute, Prandtl, thermal radiation, chemical reaction, Eckert, Schmidt, and Soret numbers, respectively.

$$\mathrm{A} = \frac{\lambda}{c}, \quad \mathrm{Kp} = \frac{\nu^*(1-\lambda t)}{k^* c}, \quad \mathrm{M} = \frac{\sigma B_0^2(1-\lambda t)}{\rho c}, \quad \mathrm{Gr} = \frac{g\beta_T x(T_w - T_\infty)cos\alpha}{u_w^2}, \quad \mathrm{Sc} = \frac{\nu^*}{D_\infty},$$
$$\mathrm{Gc} = \frac{g\beta_c x(C_w - C_\infty)cos\alpha}{u_w^2}, \quad \mathrm{Pr} = \frac{\mu Cp}{K_\infty}, \quad \mathrm{R} = \frac{16T_\infty^3\sigma^*}{3k_1 K_\infty}, \quad \mathrm{Kr} = \frac{Kc(1-\lambda t)}{c},$$
$$\mathrm{Ec} = \frac{u_w^2}{Cp(T_w - T_\infty)}, \quad \mathrm{Q} = \frac{Q'(1-\lambda t)}{c}, \quad \mathrm{So} = \frac{D_1(T_w - T_\infty)}{\nu^*(C_w - C_\infty)}, \quad (23)$$

3. Numerical Solution by Runge-Kutta Scheme

By employing the most efficient method i.e, fourth order Runge-Kutta scheme with shooting technique, from eqn. (19)-(21) we have a set of first order differential equations with seven initial problems of seven unknowns. Possible substitutions are as follows

$$f = y_1 \ , f' = y_2 \ , f'' = y_3 \ , f''' = y_3'$$
$$\theta = y_4 \ , \theta' = y_5 \ , \theta'' = y_5' \ ,$$
$$\varphi = y_6 \ , \varphi' = y_7 \ , \varphi'' = y_7' \ ,$$

The reduced equations are

$$y_3' = A\frac{\eta}{2} y_3 + [A+Kp+M]\, y_2 + y_2^2 - y_1 y_3 - Gr\, y_4 - Gc\, y_6 \quad (24)$$

$$y_5' = \frac{-\beta_1 y_5^2 + Pr\,[A(\eta/2)y_5 + 2Ay_4 + y_2 y_4 - y_1 y_5 - Ec\, y_3^2 - Ec\, Kp\, y_2^2 - Qy_4]}{(1+R+\beta_1 y_4)} \quad (25)$$

$$y_7' = \frac{-\beta_2(y_5 y_7) + Sc\,[A\left(\frac{n}{2}\right)y_7 + 2Ay_6 + y_2 y_6 - y_1 y_7 + Kry_6 - Soy_5']}{(1+\beta_2\theta)} \quad (26)$$

Corresponding Boundary conditions are given by

$y_1 = 0$, $y_2 = 1$, $y_3 = ?$

$y_4 = 1$, $y_5 = ?$, $y_6 = 1$, $y_7 = ?$

$y_1 = 0$, $y_2 = 1$, $y_3 = ?$, $y_4 = 1$, $y_6 = 1$, $y_5 = ?$, $y_7 = ?$ at $\eta = 0$

$y_2 \to 0$, $y_4 \to 0$, $y_6 \to 0$, at $\eta \to \infty$

4. Results and Discussion

This part dives into the wild world of colorful graphs and mind-boggling numbers, all relating to the non-dimensional physical parameters of the boundary value flow problem we're tackling.

All the heavy lifting in the computational department is handled by our 'MATLAB' Software. When it comes to cracking that transformed differential equation, we employ the super-effective numerical shooting technique paired with the fourth-order Runge-Kutta Scheme.

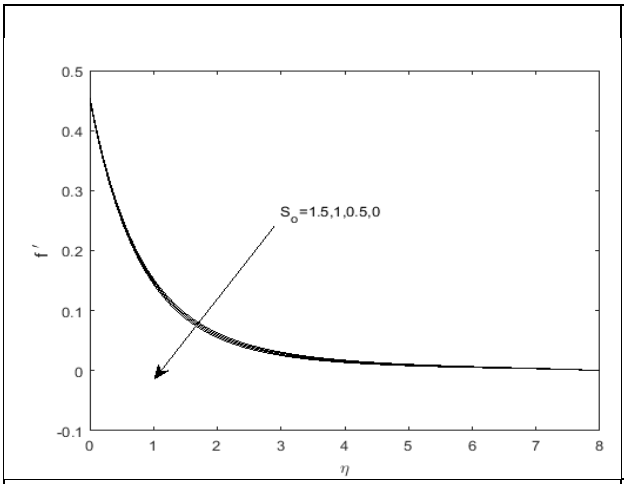

Figure 1: Effects of So on Velocity profiles When A=0.5, Kp=0.5,M=0.5,Gr=0.01,Gc=0.1

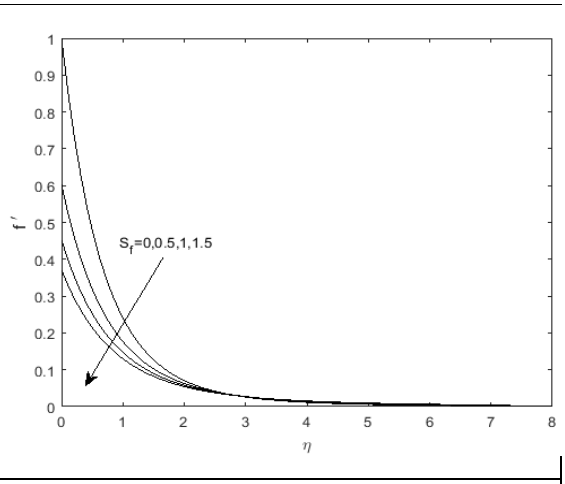

Figure 2: Effects of S_f on Velocity profiles when A=0.5, Kp=0.5,M=0.5,Gr=0.01,Gc=0.1

The Soret number (So) is like the scale that measures the drama between temperature and concentration. The larger the Soret number, the more of a diva your temperature is, flaunting a bigger difference and a steep gradient.

As the soret number increases, the velocity flow increases in the current figure 1. We may draw the conclusion that fluid flows more quickly when there is a greater temperature differential.

Again it has perceived that the alteration in velocity for several values of soret number is more exceptional at η =1 to η=3.

Fig .2. The velocity distribution in relation to the slip parameter 'S_f ' is illustrated. It is evident that the flow velocity decreases as the first-order slip parameter increases. Consequently, the slip factor becomes particularly significant when a low velocity is desired.

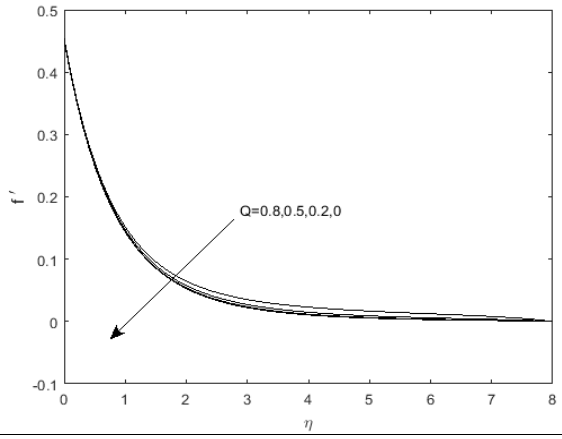

Figure 3: Effects of Thermal radiation Parameter on Velocity profiles.

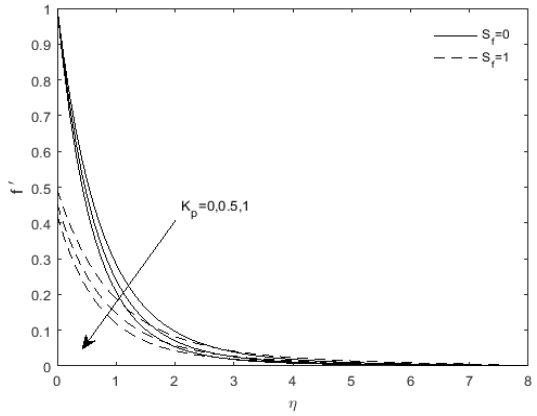

Figure 4. Effects of Porous medium parameter Velocity profiles.

In Fig 3. Velocity profiles are illustrated for varying values of the heat source parameter 'Q'. At first, the results may seem ambiguous, but once η = 1, there is a notable increase in velocity with larger heat sources. A greater heat source leads to higher velocity, indicating that the heat source acts as an assisting force.

Fig. 4 The variation in velocity profiles for different magnetic parameter values 'M' is depicted here, both with (Sf=1) and without (Sf=0) velocity slip. Thus, when the magnetic parameter is increased, the fluid flow velocity decreases. This indicates that magnetic force acts as a resistance to flow. For scientific or practical purposes, magnetic forces can be utilized to diminish flow velocity. Additionally, it is noted that the inclusion of the slip factor (S_f=1) considerably decreases the velocity compared to flow scenarios without slip.

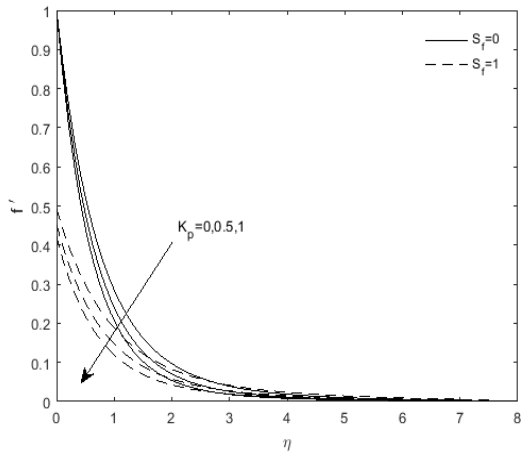

Figure 5: Effects of Porous medium Parameter on Velocity profile

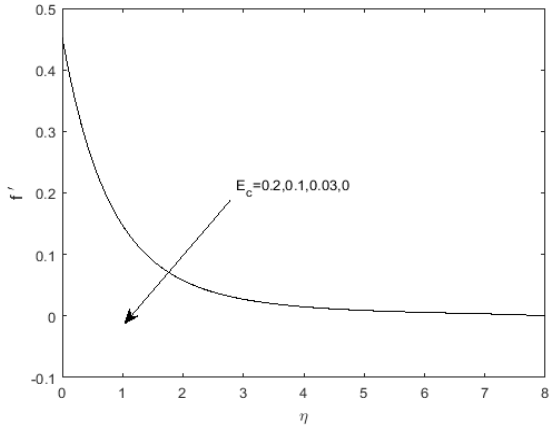

Figure 6: Effects of Eckert number on Velocity profiles.

The velocity profiles for different porosity parameter values (kp) are shown in figure 5. A trend similar to that in figure 4 can be observed, where higher kp values lead to a decrease in flow velocity. Fig.6 exhibits velocity profiles for different values of Eckert number. Ec' it is found that higher value of Eckert number enhances the velocity. But it is not so significant.

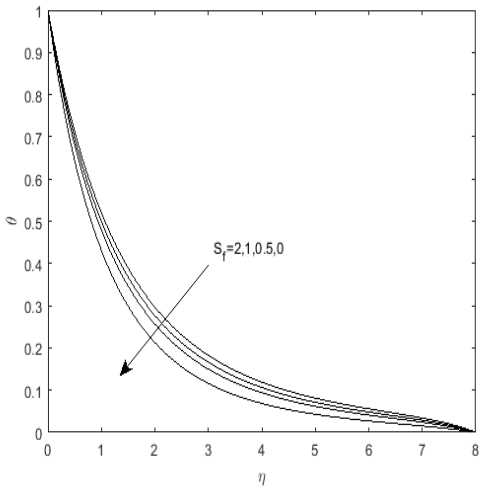

Figure 7: Effects of Slip condition on Temperature profiles

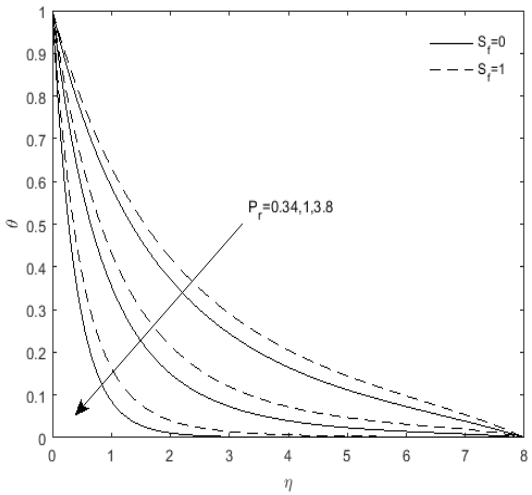

Figure 8: Effects of Prandtl number on Temperature profiles

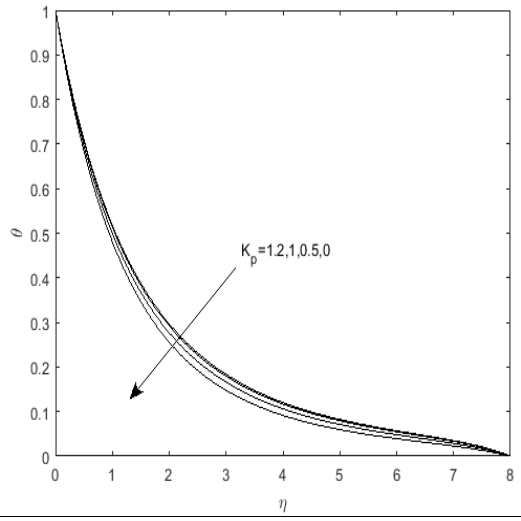

Figure 9: Effects of Porous medium parameter on Temperature profiles

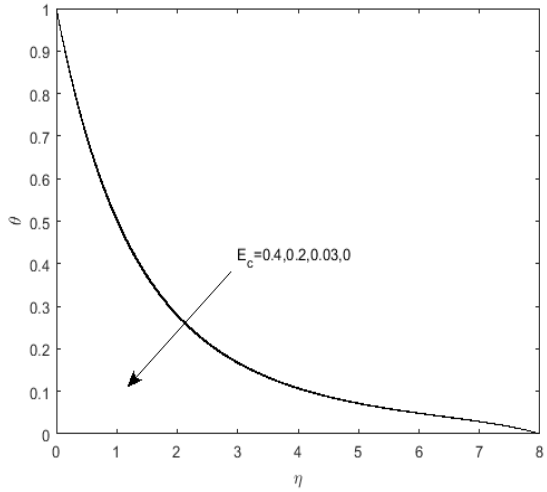

Figure 10: Effects of Eckert number on Temperature profiles.

The temperature distribution for the various prandtl number (Pr) values with and without velocity slip is shown in Fig. 7. It has been discovered that, with or without velocity slip, rising prandtl numbers lower the temperature. The ratio of momentum diffusivity to thermal diffusivity is known as the Prandtl number. Thus, it evaluates the relationship between a fluid's thermal transport capacity and momentum transport.

Higher values of Prandtl number represents lower thermal diffusivity and also the momentum transport dominates over the heat transport, which makes the fluid a poor choice for heat conduction. Therefore, lower temperature is obtained.

Further, it is clearly noticed that in presence of velocity slip, the temperature is more as compared to temperature without the slip factor. Therefore; velocity slip can be neglected when a cooling system is required.

From Fig. 8 and Fig. 9, it is observed that increasing values of both porosity parameter (kp) and Eckert number (E_c) reduce the temperature. In case of E_c, reduction of temperature is not so significant.

Fig.10 depicts the temperature profiles for some values of heat source parameter. As the heat source parameter increases, temperature increases, which is obvious.

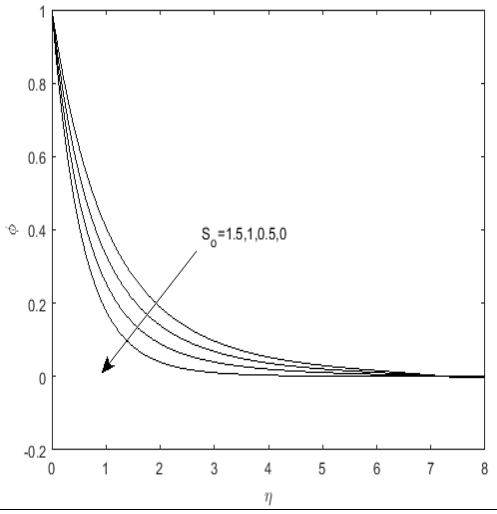

Figure 11 :Effects of Soret number on Concentration profiles

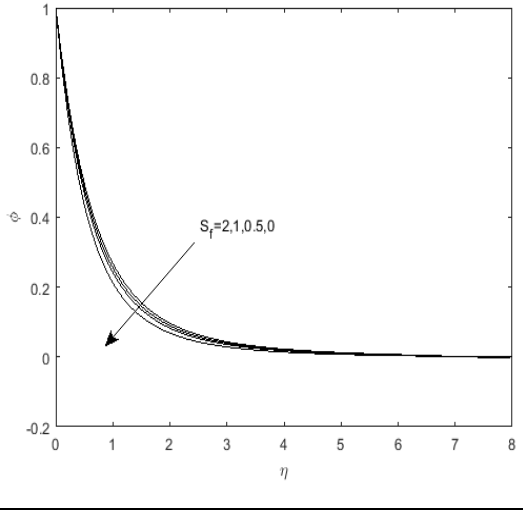

Figure 12: Effects of Slip condition on Concentration profiles

The concentration profiles for a few Soret number (So) values are shown in Fig. 11. Due to the involvement of the temperature gradient, this figure indicates that the fluid's concentration rises as the Soret number increases.

The concentration profiles for various chemical reaction parameter (Kr) values with and without velocity slip are shown in Fig. 12. It has been discovered that, in both situations—with or without velocity slip—increasing the chemical reaction parameter results in a decrease in concentration. However, compared to the concentration profile without velocity slip factor (Sf=0), concentration is found more when slip factor is present (S_f=1),

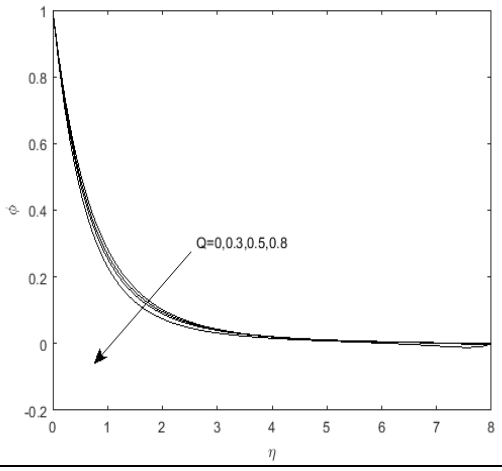

Figure 13: Effects of Thermal radiation Parameter on Concentration profiles.

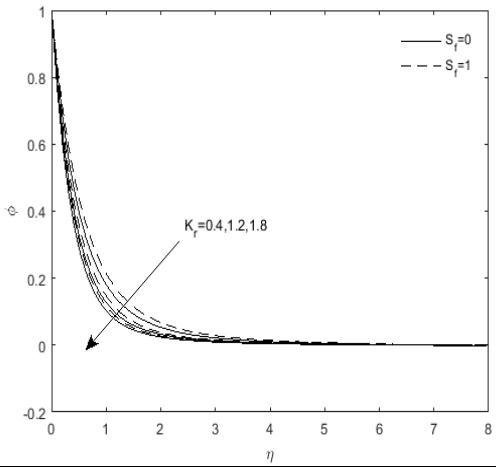

Figure 14: Effects of Chemical reaction Parameter on Concentration profiles.

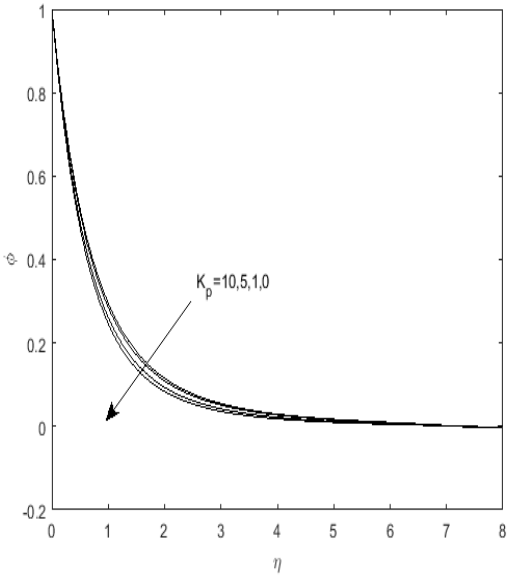

Figure 15: Effects of Porous medium parameter on Concentration profiles

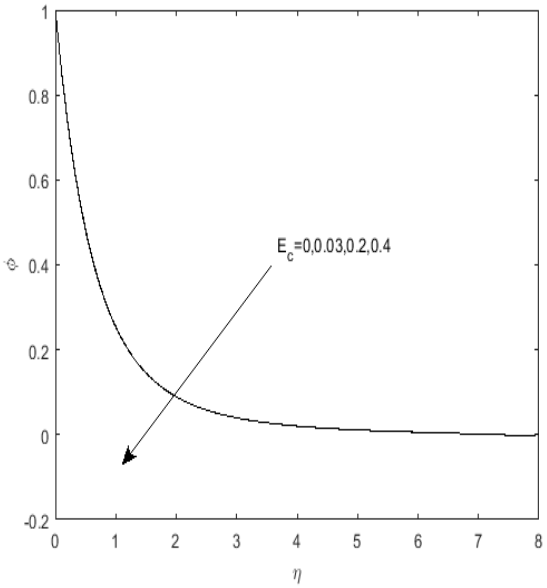

Figure 16: Effects of Eckert number on Concentration profiles

The concentration profiles for various values of the heat source parameter "Q" and the porosity parameter "Kp" are shown in Figures 13 and 15, respectively. In contrast to the porosity parameter, which is directly proportional to the concentration, the heat source parameter is inversely proportional.

Fig. 16 shows how the concentration profile is affected by the Eckert number (Ec). It has been observed that concentration improves with an increase in Eckert number.

Table 1: Comparison of $\theta'(0)$ when values of Kp = M =0.5, Gr=0.1, Gc=0.1, β_1=0.012, β_2 =0.01,P_r =0.72, R =0.01, Kr=0.1, Ec=0.03, Sc=2.

A	f_w	P_r	Gr	Ishank et.al	Sandeep et.al	B.K Swain et.al [50]	Present Study
0	-1.5	0.72	0	0.4570	0.4566	0.4570	0.4533
0	-1.5	1	0	0.5000	0.5001	0.5001	0.5000
0	-1.5	10	0	0.6452	0.6451	0.6451	0.6450
0	0	0.01	0	0.0197	0.0192	0.0197	0.1772
0	0	0.72	0	0.8086	0.8082	0.8086	0.8122
0	0	1	0	1.0000	1.0001	1.0000	1.0001
0	0	3	0	1.9237	1.9231	1.9239	1.9233
0	0	10	0	3.7207	3.7202	3.7207	3.7206
0	1.5	0.72	0	1.4944	1.4945	1.4944	1.4943
0	1.5	1	0	2.0000	2.0001	2.0000	2.0000
0	1.5	10	0	16.0842	16.0837	16.0842	16.0841
1	0	1	0	1.6820	----------	1.6820	1.6818
1	0	1	1	1.7039	----------	1.7037	1.7038

5. Conclusion

- The flow's velocity increases as the Soret number rises. From a physical point of view, fluid flows faster when the temperature differential is greater. It is evident that the velocity change for varying Soret number values is more pronounced at η = 1 to η = 3.
- As the first order slip parameter increases, the flow's velocity decreases. Therefore, whenever a low velocity is required, the slip factor is of great interest. A higher magnetic parameter lowers the fluid flow's velocity. Thus, magnetic force functions as a force that resists. Magnetic force can be used for physical or scientific purposes to lower the flow velocity. It has been discovered that a higher Eckert number increases velocity.
- With or without velocity slip, the temperature drops as the Prandtl number rises. The ratio of momentum diffusivity to thermal diffusivity is known as the Prandtl number.
- Lower thermal diffusivity and momentum transport predominate over heat transport are indicated by higher Prandtl numbers .Increasing values of both porosity parameter (Kp) and Eckert number (Ec) reduce the temperature. In case of Ec, reduction of temperature is not so significant.
- Due to the influence of the temperature gradient, the fluid's concentration rises as the Soret number does.
- It is found that increasing values of chemical reaction parameter lead to lower concentration in both the cases i.e. with or without velocity slip. But concentration in the presence of slip factor (Sf=1) is found more as compared to the concentration profile without velocity slip factor (Sf=0).
- The porosity parameter has a direct relationship with concentration, while the heat source parameter has an inverse relationship with concentration.

REFERENCES

1. S. Choi, J. Eastman (2021). Enhancing thermal conductivity of fluids with nanoparticles, (1995). https://www.osti.gov/biblio/196525 (accessed September 10, 2021).
2. M.M. Bhatti, H.F. Öztop, R. Ellahi (2022). Study of the magnetized hybrid nanofluid flow through a flat elastic surface with applications in solar energy, Materials (Basel). 15, 7507.
3. S.M. Hussain, W. Jamshed, R. Safdar, F. Shahzad, N.A.A. Mohd Nasir, I. Ullah (2023). Chemical reaction and thermal characteristiecs of Maxwell nanofluid flow-through solar collector as a potential solar energy cooling application: A modified Buongiorno's model, Energy Environ. 34, 1409–1432.

4. M.R. Eid, M.A. Nafe (2022). Thermal conductivity variation and heat generation effects on magneto-hybrid nanofluid flow in a porous medium with slip condition, Waves in Random and Complex Media. 32, 1103–1127.

5. S.A. Lone, M.A. Alyami, A. Saeed, A. Dawar, P. Kumam, W. Kumam (2022). MHD micropolar hybrid nanofluid flow over a flat surface subject to mixed convection and thermal radiation, Sci. Rep. 12, 1–14.

6. H. Waqas, U. Farooq, D. Liu, M. Abid, M. Imran, T. Muhammad (2022). Heat transfer analysis of hybrid nanofluid flow with thermal radiation through a stretching sheet: A comparative study, Int. Commun. Heat Mass Transf. 138, 106303.

7. K.A.M. Alharbi, Adnan, M.Z. Bani-Fwaz, S.M. Eldin, A. Akgul (2023). Thermal management in annular fin using ternary nanomaterials influenced by magneto-radiative phenomenon and natural convection, Sci. Rep. 13, 9528.

8. I.L. Animasaun, Q.M. Al-Mdallal, U. Khan, A.S. Alshomrani (2022). Unsteady Water-Based Ternary Hybrid Nanofluids on Wedges by Bioconvection and Wall Stretching Velocity: Thermal Analysis and Scrutinization of Small and Larger Magnitudes of the Thermal Conductivity of Nanoparticles, Mathematics. 10, 4309.

9. M.Z. Bani-Fwaz, Z. Mahmood, M. Bilal, A.A. EI-Zahhar, I. Khan, S. Niazai (2024). Computational Investigation of thermal process in radiated nanofluid modulation influenced by nanoparticles (Al2O3) and molecular (H2O) diameters, J. Comput. Des. Eng. 11, 22–36.

10. S.K. Rawat, S. Negi, H. Upreti, M. Kumar (2021). A non-Fourier's and non-Fick's approach to study MHD mixed convective copper water nanofluid flow over flat plate subjected to convective heating and zero wall mass flux condition, Int. J. Appl. Comput. Math. 7, 1–27.

11. M.N. Abrar (2014). Entropy analysis of double diffusion in a Darcy medium with tangent hyperbolic fluid and slip factors over a stretching sheet: Role of viscous dissipation, Numer. Heat Transf. Part A Appl. 1–14.

12. M. Sheikholeslami, D.D. Ganji (2016). Nanofluid convective heat transfer using semi analytical and numerical approaches: a review, *J. Taiwan Inst. Chem. Eng.* 65, 43–77,

13. O. Ghaffarpasand (2016). Numerical study of MHD natural convection inside a sinusoidally heated lid-driven cavity filled with Fe3O4-water nanofluid in the presence of Joule heating, *Appl. Math. Model*. (2016).

14. B. Mahanthesh, B.J. Gireesha, R.S.R. Gorla (2016). Unsteady three dimensional MHD flow of a nano Eyring-Powell fluid past a convectively heated stretching sheet in the presence of thermal radiation, viscous dissipation and Joule heating, *J. Ass. Arab Univ. Bas. Appl. Sci*. (2016).

15. Mohsen Sheikholeslami, Davood Domiri Ganji, (2015). Nanofluid flow and heat transfer between parallel plates considering Brownian motion using DTM, *Comput. Methods Appl. Mech. Eng*. 283, 651–663.

16. S. Saleem, I.L. Animasaun, S.-J. Yook, Q.M. Al-Mdallal, N.A. Shah, M. Faisal (2022). Insight into the motion of water conveying three kinds of nanoparticles shapes on a horizontal surface: Significance of thermo migration and Brownian motion, Surfaces and Interfaces. 30, 101854.

17. W. Cao, I.L. Animasaun, S.-J. Yook, V.A. Oladipupo, X. Ji (2022). Simulation of the dynamics of colloidal mixture of water with various nanoparticles at different levels of partial slip: Ternary-hybrid nanofluid, Int. Commun. Heat Mass Transf. 135, 106069.

18. M.N. Abrar, W. Yun, M. Sharaf (2024). Entropy generation due to MHD Falkner–Skan flow of Casson fluid over a wedge: A numerical study, ZAMM-Journal Appl. Math. Mech. Für Angew. Math. Und Mech. e202300750.

19. Y. Khan, S. Akram, A. Razia, A. Hussain, H.A. Alsulaimani, (2022). Effects of double diffusive convection and inclined magnetic field on the peristaltic flow of fourth grade nanofluids in a non-uniform channel, *Nanomaterials*. 12, 3037.

20. M. Mohammadi, S.A.G. Nassab, (2022). Combined influences of radiation and inclined magnetic field on natural convection in a cavity with complex geometry, Int. Commun. Heat Mass Transf. 134, 106030.

21. Q. Khan, M. Farooq, S. Ahmad (2024). Generalized transport analysis on mixed convection squeeze flow of a Casson fluid over an inclined stretching sheet with viscous dissipation and double stratification, Ain Shams Eng. J. 15, 102253.

22. S. Nadeem, Rashid Mehmood, S.S. Motsa, (2015). Numerical investigation on MHD oblique flow of Walter's B type nanofluid over a convective surface, *Int. J. Therm.Sci.* 92, 162–172.

23. C.S.K. Raju, N. Sandeep, V. Sugunamma, M. Jayachandra Babu, J.V. Ramana Reddy (2016). Heat and mass transfer in magneto hydrodynamic Casson fluid over an exponentially permeable stretching surface, *Eng. Sci. Technol. Int. J.* 19, 45–52.

24. Kai-Long Hsiao (2017). Micropolar nanofluid flow with MHD and viscous dissipation effects towards a stretching sheet with multimedia feature, *Int. J. Heat Mass Transf.* 112, 983–990.

25. S.S. Ghadikolaei, Kh Hosseinzadeh, M. Yassari, H. Sadeghi, D.D. Ganji (2017). Boundary layer of micropolar dusty fluid with Tio2 nanoparticles in a porous medium under the effect of magnetic field and thermal radiation over a stretching sheet, *J. Mol. Liq.* 244, 374-389.

26. M. Ramzan, N. Shahmir, C.A. Saleel, S. Kadry, S.M. Eldin, A.M. Saeed (2023). Model-based comparison of hybrid nanofluid Darcy-Forchheimer flow subject to quadratic convection and frictional heating with multiple slip conditions, Numer. Heat Transf. Part A Appl. (2023), 1–21.

27. S.A.S. Al Rashdi, N.I. Ghoneim, A.M. Amer, A.M. Megahed, (2023). Investigation of magnetohydrodynamic slip flow for Maxwell nanofluid over a vertical surface with Cattaneo-Christov heat flux in a saturated porous medium, Results Eng. 19, 101293.

28. S.S. Ghadikolaei, Kh Hosseinzadeh, D.D. Ganji, M. Hatami (2018). Fe3O4–(CH2OH)2 nanofluid analysis in a porous medium under MHD radiative boundary layer and dusty fluid, *J. Mol. Liq.* 258, 172–185.

29. M. Hatami, Kh Hosseinzadeh, D.D. Ganji, M.T. Behnamfar (2014). Numerical study of MHD two-phase Couette flow analysis for fluid-particle suspension between moving parallel plates, *J. Taiwan Inst. Chem. Eng.* 45, 2238–2245.

30. S.M. Ibrahim, G. Lorenzini, P. Vijaya Kumar, C.S.K. Raju, (2017). Influence of chemical reaction and heat source on dissipative MHD mixed convection flow of a Casson Nanofluid over a nonlinear permeable stretching sheet, *Int. J. Heat Mass Transf.* 111, 346–355.

31. S.S. Ghadikolaei, Kh Hosseinzadeh, D.D. Ganji, (2017). Analysis of unsteady MHD Eyring-Powell squeezing flow in stretching channel with considering thermal radiation and Joule heating effect using AGM, Case Stud. *Therm. Eng.* 10, 579–594.

32. Umar Khan, Naveed Ahmed, Syed Tauseef Mohyud-Din (2017). Numerical investigation for three-dimensional squeezing flow of nanofluid in a rotating channel with lower stretching wall suspended by carbon nanotubes, *Appl. Therm. Eng.* 113, 1107–1117.

33. B. Mahanthesh, B.J. Gireesha, R.S.R. Gorla (2016). Nonlinear radiative heat transfers in MHD three dimensional flow of water based nanofluid over a non-linearly stretching sheet with convective boundary condition, *J. Niger. Math. Soc.* 35, 178–198.

34. Ramesh GK, Prasannakumara BC, Gireesha BJ, Rashidi MM. (2016). Casson fluid flow near the stagnation point over a stretching sheet with variable thickness and radiation. *J Appl Fluid Mech,* 9(3), 1115–22.

35. E. Haile and B. Shankar. (2014). Heat and mass transfer through a porous media of mhd flow of nanofluids with thermal radiation, viscous dissipation and chemical reaction effects. *American Chemical Science Journal,* 4, 828-846.

36. Kar S. Senapati N. Swain B.K. (2019). Effect of chemical reaction on MHD flow with heat and mass transfer past a vertical porous plate in the presence of viscous dissipation. *International Journal of Advances in Applied Sciences (IJAAS), 8(1), 83-94.*

37. Kar. S, Swain. B.K, Senapati N and Dash M (2021). The effect of viscous dissipation and low pressure gradient on a Magnetohydrodynamics flow over a flat plate". *Mathematical Modelling of Engineering Problems, 8(2), 285-292.*

38. Chen CH. (2010). On the analytic solution of MHD flow and heat transfer for two types of viscoelastic fluid over a stretching sheet with energy dissipation, internal heat source and thermal radiation. *Int.J.Heat Mass Transfer.* 53, 4264-73.

39. S. Ahmed, A. Batin and A.J Chamkha (2014). Finite Difference Approach in porous media transport modelling for Magneto hydrodynamic unsteady flow over a vertical plate: Darcian Model, *Int. J. of Numerical Methods for Heat and Fluid Flow*, 24(5), 1204-1223.

40. S Ahmed and A.J. Chamkha (2014). Hartmann Newtonian Radiating MHD flow for a rotating vertical porous channel immersed in a Darcian porous regime: An exact solution, *Int. J. of Numerical Methods for Heat and Fluid Flow,* 24(7), 1454-1470.

41. Senapati .N, Dhal R.K, Das T.K, (2012). Effects of chemical reaction on mass and heat transfer on MHD free convection flow of fluids in vertical plates and in between parallel plates for slips flow regions, *American Journal of Computational and Applied mathematics*, 2(3), 124-135.

42. Paul A. (2017). Transient free convective MHD flow past an exponentially accelerated vertical porous plate with variable temperature through a porous medium, *International Journal of Engineering Mathematics,* Article ID2981071, 1-9.

43. T. Hayat, M. Mustafa and I. Pop (2010). Heat and mass transfer for Soret and Dufour effects on mixed convection boundary layer flow over a stretching vertical surface in a porous medium filled with a visco-elastic fluid, *Communications in Nonlinear Science and Numerical Simulation,* 15 (5), 1183 – 1196

44. Yih KA (1997). The effect of transpiration on coupled heat and mass transfer in mixed convection over a vertical plate embedded in a saturated porous medium. *International Communications in Heat and Mass Transfer,* 24(2), 265–275.

45. B.K.Swain, B.C.Parida, S.Kar, N.Senapati (2020). Viscous dissipation and joule heating effect on MHD flow and heat transfer past astretching sheet embedded in a porous medium, *Journal of Heliyon, 1 (3), 1-8.*

46. K. Saeed, S. Akram, A. Ahmad, M. Athar, M. Imran, T. Muhammad, (2022). Impact of partial slip on double diffusion convection and inclined magnetic field on peristaltic wave of six-constant Jeffreys nanofluid along asymmetric channel, Eur. Phys. J. Plus. 137, 364.

47. Q. Khan, M. Farooq, S. Ahmad, (2021). Convective features of squeezing flow in nonlinear stratified fluid with inclined rheology, Int. Commun. Heat Mass Transf. 120, 104958.

48. A.M. Amer, S.A.S. Al Rashdi, N.I. Ghoneim, A.M. Megahed, (2023).Tangent hyperbolic nanofluid flowing over a stretching sheet through a porous medium with the inclusion of magnetohydrodynamic and slip impact, Results Eng. 19, 101370.

49. K. Srihari, J. Anand Rao and N. Kishan : MHD free convection flow of an incompressible viscous dissipative fluid in an infinite vertical oscillating plate with constant heat flux, Journal of Energy, Heat and Mass Transfer, 28,(2006), pp.19-28.

50. B.K.Swain,S.Kar : Dissipative MHD flow of ternary-hybrid nanofluid over an inclined stretching sheet with heat source and mass flux due to temperature gradient, Journal of applied mathematics and Mechanics, *Z Angew Math Mech.* 2024;e202200360. https://doi.org/10.1002/zamm.202200360.

****